Pumping new life into preclinical pharmacokinetics: exploring the pharmacokinetic application of ex vivo organ perfusion

Stevens, L.J.

CHAPTER 04

Novel explanted human liver model to assess hepatic extraction, biliary excretion and transporter function

L.J. Stevens, J. Dubbeld, J.B. Doppenberg, B. Van Hoek, A.L. Menke, J.M. Donkers, A. Alsharaa, A. De Vries, W.H.J. Vaes, C.A.J. Knibbe, E. van de Steeg, I.P.J. Alwayn

Clinical Pharmacology & Therapeutics, 2023

Abstract

Realistic models predicting hepatobiliary processes in health and disease are lacking. We therefore aimed to develop a physiologically relevant human liver model consisting of normothermic machine perfusion (NMP) of explanted diseased human livers that can assess hepatic extraction, clearance, biliary excretion and drug-drug interaction

Eleven livers were included in the study, seven with a cirrhotic and four with a non-cirrhotic disease background. After explantation of the diseased liver, NMP was initiated. After 120 minutes of perfusion, a drug cocktail (rosuvastatin, digoxin, metformin and furosemide; OATP1B1/1B3, Pgp, BCRP and OCT1 model compounds) was administered to the portal vein and 120 minutes later, a second bolus of the drug cocktail was co-administered with perpetrator drugs to study relevant drug-drug interactions.

The explanted livers showed good viability and functionality during 360 minutes of NMP. Hepatic extraction ratios close to *in vivo* reported values were measured. Hepatic clearance of rosuvastatin and digoxin showed to be the most affected by cirrhosis with an increase in Cmax of 11.50 and 2.89 times, respectively, compared to non-cirrhotic livers. No major differences were observed for metformin and furosemide. Interaction of rosuvastatin or digoxin with perpetrator drugs were more pronounced in non-cirrhotic livers compared to cirrhotic livers.

Our results demonstrated that NMP of human diseased explanted livers is an excellent model to assess hepatic extraction, clearance, biliary excretion and drug-drug interaction. Gaining insight into pharmacokinetic profiles of OATP1B1/1B3, Pgp, BCRP and OCT1 model compounds is a first step towards studying transporter functions in diseased liver.

Introduction

Accurate prediction of drug disposition in patients with and without hepatic diseases remains difficult, as appropriate models are lacking. The liver plays an important role in drug handling and impairment or alteration of its function may greatly affect multiple processes. Upon first liver pass, after oral administration, drug bioavailability as well as drug clearance may be altered thereby affecting the drug's efficacy. Studies in liver cirrhosis have shown that increased bioavailability as well as reduced clearance lead to a higher prevalence of adverse drug reactions and drug-drug interactions which can result in safety issues and ultimately an increased risk for hospital admission[1,2]. Therefore, drug dosing should be tailored according to the varying degree of liver dysfunction among patients with liver diseases. However, with the currently available preclinical and clinical models, it remains difficult to quantify the required tailoring of the dose related to the degree and type of liver dysfunction[3].

Established *in vitro* and animal models are often used to study the pathology and pharmacological characteristics of drugs of varying diseases. However, translation of these findings to clinical practice remains challenging due to, among others, species differences in transporter expression and the difficulty to mimic dynamic liver processes[4,5]. Novel 3D models like liver-on-a-chip and bile duct-on-a-chip models have gained significant interest as a predictive platform to study liver processes due to the incorporation of haemodynamics[6,7]. Although these organ-on-a-chip models hold much promise, they are still in their infancy owing to the difficulty of mimicking (patho)physiological processes in the liver such as portal and arterial blood flow and biliary excretion[7]. Normothermic machine perfusion (NMP) systems using human *ex vivo* whole organs overcome this problem since hepatic architecture is combined with (near) physiological hemodynamics. Thereby, use of human explanted liver whole organ enables to study hepatobiliary processes as well as liver disease specific pharmacokinetics[8-10].

In this study we developed a novel hepatic model using diseased explanted human livers. Four model drugs (rosuvastatin, digoxin, furosemide and metformin) with and without perpetrator drugs were used to study hepatic extraction, clearance, biliary excretion and drug-drug interaction. These model

drugs are known substrates for different important hepatic uptake and efflux transporters and enabled comparison of the model to *in vivo* reported data.

Materials and methods

Human livers

Patients undergoing liver transplantation were included in this study. After providing informed consent, the patients approved the usage of the explanted liver for experimental study (Figure 4.1). The use of explanted liver tissue was approved by the medical ethical committee of the Leiden University Medical Center (B19.040). Patients with polycystic liver disease, with a transjugular intrahepatic portosystemic shunt, or waitlisted for recurrent- orthotopic liver transplantation were excluded from participation. Eleven human livers were included in the study. The underlying disease processes of these livers were primary biliary cholangitis (PBC, n=1), non-alcoholic fatty liver disease (NAFLD, n=2), alcoholic liver disease (ALD, n=3), hepatocellular carcinoma in the context of Hepatitis B viral disease (HBV+HCC, n=2). In addition, three discarded non-cirrhotic livers which were declined for transplantation were included in this study. The reasons for decline were; steatosis (n=2) and an occlusion of right hepatic artery (n=1). Immediately following explantation of the recipient diseased liver, a portal and arterial flush with cold Histidine-tryptophan-ketoglutarate (HTK) (Carnamedica, Warsaw, Poland) preservation solution was performed. The period between explantation (i.e. clamping and transection of the portal and hepatic veins as final step of the hepatectomy) and cold flush of the explanted liver (*ex vivo*), is described as the warm ischemia time (WIT). After a clean effluent flush, the liver was transported in cold preservation solution to the Organ Preservation and Regeneration room in the OR complex. Here, under sterile conditions, a back table reconstruction of the right and left hepatic artery and portal vein was performed using surplus donor blood vessels, in order to facilitate cannulation (portal vein- 25Fr cannula, hepatic artery – 12Fr cannula) and connection to the machine perfusion device (Liver Assist™ device, XVIVO, Groningen, the Netherlands). Thereafter, the bile duct was cannulated.

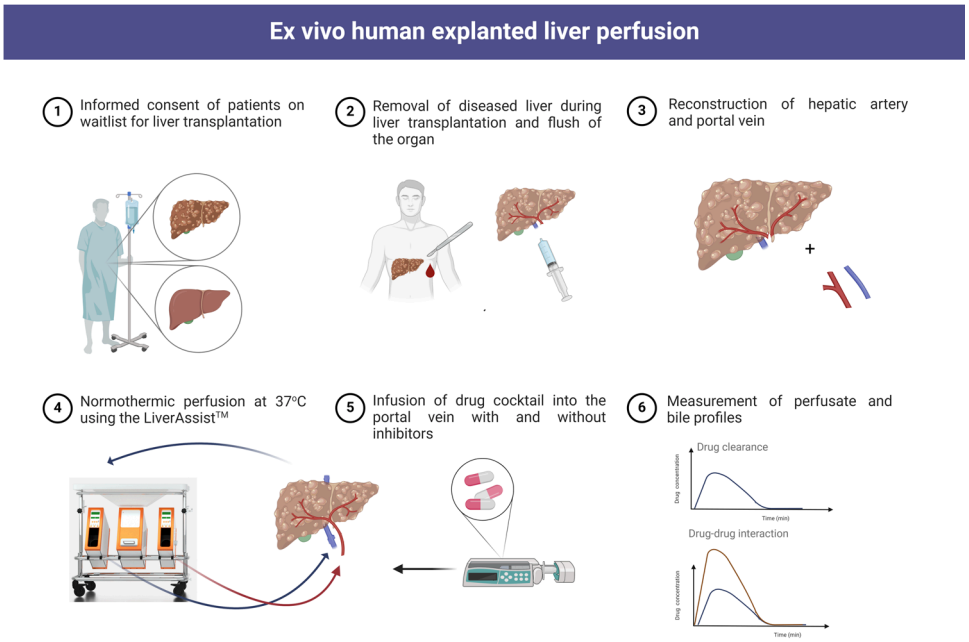

Figure 4.1 - Schematic representation of normothermic explanted human liver perfusion set-up.

Normothermic machine perfusion

All human livers were perfused using the Liver Assist™ device. The machine consists of two centrifugal pumps which provide a pulsatile flow to the hepatic artery and a continuous flow to the portal vein[11]. The system reservoir was filled with 2L perfusion fluid containing 1:1 ratio of human red blood cells and fresh frozen plasma (Sanquin, Amsterdam, the Netherlands). Insulin, sodium taurocholate, heparin and epoprostenol were provided as continuous infusion at a rate of 10U/h, 1041U/h, 10 mL/h (2% w/v) and 8 µg/h, respectively, in order to maintain liver functioning and to facilitate bile flow. Additionally, nutrients (aminoplasmal 10E (B Braun Melsungen AG, Melsungen, Germany) and cernevit (Baxter BV, Utrecht, the Netherlands) were continuously provided (23mL/hr) to keep the liver metabolically active (Supplemental Table S4.1). Gas delivery to the Liver Assist™ consisted of 95% oxygen and 5% carbon dioxide at 1.5 L/min and the temperature was set at 37°C. The non-cirrhotic livers were perfused with a portal pressure of 11 mmHg and the cirrhotic livers required perfusion at 14 mmHg to generate a sufficient portal flow. Mean arterial pressure was set at 50 mmHg. After 360 minutes of perfusion, the livers were submerged in

formaldehyde and transported the pathology department and were examined according to the institution's clinical guidelines dependent on the patient's underlying pathophysiology.

Drug administration during perfusion

Drug clearance in perfusate and bile of the drug cocktail (rosuvastatin, metformin, furosemide and digoxin) were determined in the absence and presence of perpetrator drugs (quinidine, rifampicin, cimetidine and probenecid)[12]. The dosage applied to the system were based on clinically prescribed oral dosage and calculated as previously described in Stevens et al. 2021[13]. In short, portal doses of the drug cocktail compounds and inhibitors were calculated based on the fraction absorbed in the intestine to the portal vein, fraction of metabolism and circulating volume (Supplemental Table S4.2). After 120 min. of perfusion, a slow bolus for 10 min of the drug cocktail was administered via the portal vein at 1 mL/min to mimic oral absorption through the gut. Subsequently, perfusate and bile samples were taken for the following 120 min. Arterial samples were taken at t=120, 122, 124, 126, 128, 130, 135, 140, 150, 160, 170, 180, 210, and 240 min. Additional portal samples were taken during the administration of the drug at t=126 and t=130 min to determine the hepatic extraction. Bile samples were collected in 10 minute fractions from 120 min onwards. After 240 min., first a slow bolus 10 min (1 mL/min) of perpetrator drugs (quinidine, cimetidine, rifampicin and probenecid) was administered to the liver and after 5 min (at t=245 min.), again, a subsequent slow bolus of the drug cocktail was administered via the portal vein. Biopsies were taken at the end of the first dose (t=240 min) and second dosing with inhibitors (t=360 min). The same sampling schedule for arterial samples and bile samples was followed. Perfusate and bile samples were immediately stored at ≤-70°C until further processing.

Liver function assessment

Hepatic artery and portal vein flow were recorded from the Liver Assist™ machine. Perfusate samples and bile samples (collected under mineral oil to prevent bile exposure to ambient air[14]) were taken hourly to monitor liver viability (pH, glucose, lactate etc.) using a RapidPoint 500 blood gas analyzer (Siemens, Germany). Alanine aminotransferase (ALT) concentration in the perfusate samples was measured by reflectance photometry (Reflotron-Plus system, Roche diagnostics, Almere, the Netherlands). Perfusate and bile

parameters were compared to defined criteria used in clinical transplantation studies; perfusate ALT <6000 and lactate <2.5 mmol/L after 120 min of perfusion, biliary pH >7.5 (15-17).

Histological analysis

Pre-perfusion (n=2) and post-perfusion (n=2) biopsies were taken for each liver, fixed in 10% formalin and subsequently embedded in paraffin. Slices of 4 µm were cut and stained with hematoxylin & eosin (H&E) for examination using light microscopy.

Bioanalysis

The concentration of the drug cocktail was quantified using LC-MS/MS (Waters, Etten-Leur, the Netherlands). Perfusate and bile sample (10 µL) were deproteinized with 100 µL acetonitrile (ACN) with the addition of 10 of µL the isotopically labelled internal standards (1 µg/mL). Thereafter samples were vortexed, centrifuged and supernatant was transferred to 96 well plate and dried under nitrogen. Thereafter, samples were dissolved in 100 µL 10% ACN + 0,1% formic acid and injected in to LC-MS/MS for quantification. Details of the LC-MS/MS conditions used are shown in Supplemental Table S4.3 and S4.4.

Chemicals

Rosuvastatin, digoxin, furosemide, quinidine were obtained from Sigma-Aldrich (Zwijndrecht, the Netherlands). Metformin and rifampicin and cimetidine were obtained from Bioconnect (Huissen, the Netherlands). Heparin, sodium taurocholate (Sigma-Aldrich, Zwijndrecht, the Netherlands), insulin (Novo Nordisk, Alphen aan den Rijn, the Netherlands) and epoprostenol (Flolan; GlaxoSmithKline Inc, Mississauga, ON, Canada) were obtained as indicated.

Data analysis and statistics

Data obtained during the perfusion studies was analyzed using Prism version 8 (GraphPad, California, USA). Values for the area under the concentration time curve 0 -120 min ($AUC_{0\text{-}tau}$) were calculated using the linear trapezoidal method. The area under the concentration time curve ratio (AUCR) was determined by dividing the $AUC_{125\text{-}245\ min}$ (with inhibitors) by the $AUC_{0\text{-}120\ min}$ (without inhibitors). The hepatic extraction ratio was calculated during the 10 min dosing period as following: concentration entering the liver (portal vein) - concentration leaving

the liver / concentration entering the liver. Significance of differences between the cirrhotic and non-cirrhotic livers was tested using the Mann-Whitney U test. Data is presented as median and inter-quartile range (IQR) for non-parametric distributed data. P-value below 0.05 was considered significant.

Results

Explanted livers showed good viability during perfusion

Both cirrhotic (n=7, characteristics Table 4.1) and non-cirrhotic (n=4, characteristics Table 4.1) livers had a stable arterial flow with minimal variation during perfusion; 235 mL/min (IQR:214.7-249) in cirrhotic livers vs. 230 mL/min (IQR:21.3-239.5) in non-cirrhotic livers (Figure 4.2A). A significant lower portal flow in cirrhotic livers was observed compared to non-cirrhotic livers of 523 mL/min (IQR:489-557) vs. 1678 mL/min (IQR:1596-1710)), respectively, $p<0.001$ (Figure 4.2B). Figure 4.2C demonstrates perfusate lactate, which is a marker of liver function. Lactate clearance was observed after 30 min of perfusion in the non-cirrhotic liver group and remained low (1.39 mmol/L (IQR:0.48-.29)), while cirrhotic livers showed higher levels of perfusate lactate (13.25 mmol/L (IQR:3.20-22.91) after 360 min of NMP). As marker of hepatocellular injury, release of ALT was measured throughout the perfusion (Figure 4.2D). Levels of ALT reached a plateau after 60 min of perfusion and remained stable until 360 min of perfusion. ALT levels were significantly higher in the non-cirrhotic livers compared to the cirrhotic livers ($p=0.017$). All livers produced bile during perfusion, but significantly more bile was produced by the cirrhotic livers 55 mL (IQR:37-61) vs. 28 mL (IQR:22-60)) $p=0.034$ (Figure 4.2E). The pH of produced bile during perfusion showed to be >7.5 in cirrhotic as well as non-cirrhotic livers (Figure 4.2F), demonstrating good cholangiocyte viability and meeting the defined viability criteria. To investigate the effect of perfusion on the integrity of the livers, biopsies of the livers pre-, and post-perfusion were stained with H&E. Figure 4.2G shows a representative example of a non-cirrhotic liver and a cirrhotic liver, before perfusion and post-perfusion (t=360 min). The histopathological analysis indicated that the perfusion did not have obvious detrimental morphological effects on the liver tissue. Additional markers of hepatocellular injury and function and cholangiocyte viability can be found in Supplemental Figure S4.1. Gene expression data of housekeeping genes, transporters and enzymes can be found in Supplemental Figure S4.2.

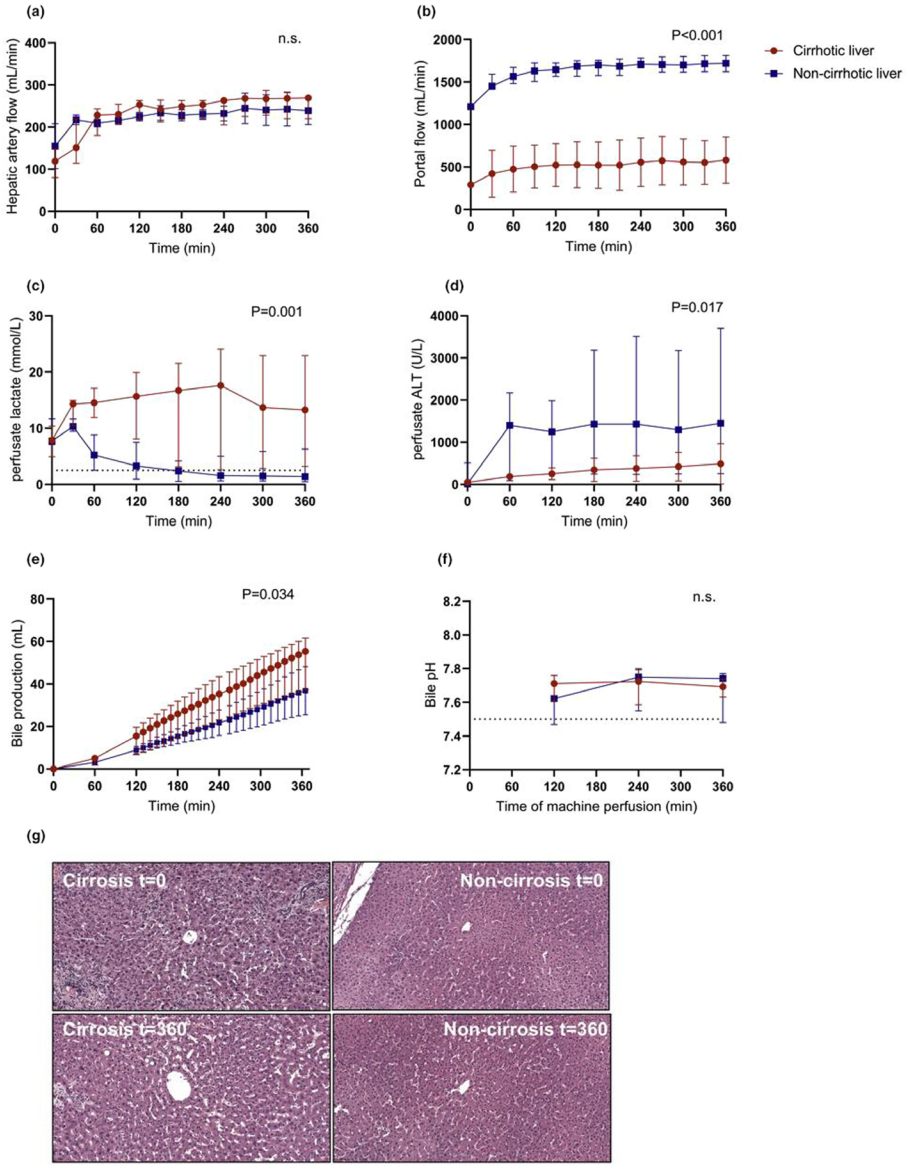

Figure 4.2 - Liver functionality, viability, and injury markers measured in perfusate, bile, and tissue of normothermic perfused cirrhotic and noncirrhotic livers. (a) hepatic artery flow, (b) portal flow, (c) perfusate lactate, (d) perfusate ALT levels (e) bile production (f) biliary pH and of cirrhotic and noncirrhotic livers measured during 360 minutes of normothermic perfusion. (g) H&E staining of a cirrhotic liver and noncirrhotic liver, before perfusion (t=0) and after perfusion (360 minutes; 200×). Data represent median and interquartile range in cirrhotic (n=7) and noncirrhotic livers (n=4). Differences between groups were analyzed using the Mann–Whitney U test; P value is presented in the right corner of each graph. ALT, alanine aminotransferase; H&E, hematoxylin and eosin; n.s., not significant.

Table 4.1 - Liver characteristics and ischemic times of cirrhotic and non-cirrhotic livers.

	Cirrhotic livers *N*=7	Noncirrhotic livers *N*=4	*P* values
Underlying disease	ALD (*n*=3) NAFLD (*n*=2) HBV+HCC (*n*=1) PBC (*n*=1)	Discarded liver (*n*=3) HBV+HCC (*n*=1)	n.a.
Age, years	59 (54–69)	63 (30–67)	0.545
Gender			
Male	6	4	
Female	1	0	
BMI, kg/m^2	29.4 (23.8–31.4)	26.8 (26.0–28.8)	>0.99
WIT, minutes	5 (4–6)	12 (5–14)	0.067
CIT, minutes	80 (71–99)	270 (105–507)	0.070
Weight of the liver, g	1,507 (1,297–2,005)	1,975 (1,394–2,008)	0.648
MELD	11 (9–23)	6 (6–6)	0.006

Differences between groups were analyzed using the Mann–Whitney U test. ALD, alcoholic liver disease; BMI, body mass index; CIT, cold ischemia time; HBV, hepatitis B virus; HCC, hepatocellular carcinoma; MELD, model of end stage liver disease; n.a., not applicable; NAFLD, nonalcoholic fatty liver disease; PBC, primary biliary cholangitis; WIT, warm ischemia time..

Hepatic clearance and biliary excretion of rosuvastatin and digoxin are affected by cirrhosis

To assess hepatic clearance and biliary excretion, a drug cocktail was infused to the portal vein (Figure 4.3, Supplemental Figure S4.3, Supplemental Table S4.1). Perfusate concentrations of rosuvastatin appeared to be the most affected by liver cirrhosis, with an approximate 11.5-fold increased Cmax in cirrhotic livers compared to the perfused non-cirrhotic livers (463.3 ng/mL (IQR: 243.2-555.2) vs. 41.10 ng/mL (IQR: 7.01-71.02), p=0.024) and 190-fold increased $AUC_{0\text{-}tau}$ of 20.96 µg/mL (IQR: 11.61-29.98) vs. 0.11 µg/mL (IQR:0.10-5.15, p<0.001) (Figure 4.4A). A comparable effect was observed for digoxin, with a perfusate Cmax that was more than 3-fold higher in cirrhotic livers (10.03 ng/mL (IQR:7.75-11.78)) compared to non-cirrhotic livers (3.46 ng/mL ng/mL (IQR:2.33-7.80, p=0.038)) and an $AUC_{0\text{-}tau}$ that was almost 3-fold higher; 629 ng/mL (IQR:282-746) in cirrhotic livers versus 222 ng/mL (IQR:171-503) in non-cirrhotic livers, p=0.003 (Figure 4.4D). Biliary excretion of rosuvastatin and digoxin was higher in cirrhotic livers (66% and 51% respectively) compared to non-cirrhotic livers (47% and 17%, respectively), however not significant (Figure 4.4B,E). Figure 4.4C and 4.4F show lower intrahepatic levels of rosuvastatin and digoxin respectively in cirrhotic livers compared to non-cirrhotic livers which is in line with the biliary excretion. As can be observed in Figure 4.4G-L, cirrhosis had a minor effect on furosemide and metformin concentrations as Cmax was 1.19 and 1.13 times higher in cirrhotic livers compared to non-cirrhotic livers (not significant). Metformin and furosemide were only minimally cleared through biliary

excretion (in the range of 1-3%) which was not affected by the cirrhosis (Figure 4.4H,K) and also intrahepatic levels were comparable between cirrhotic and noncirrhotic livers (Figure 4.4I,L).

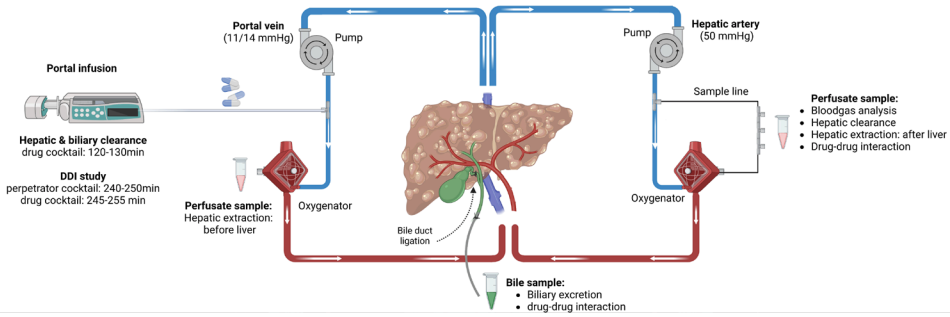

Figure 4.3 - Schematic representation of normothermic machine perfusion setup of the liver to study drug hepatobiliary processes. DDI, drug-drug interaction.

Hepatic extraction of rosuvastatin affected by cirrhosis

A unique application of the perfusion model is to sample from the portal vein (before the liver) and hepatic artery (after liver sample) during the dosing period (Figure 4.5A), enabling to determine the hepatic extraction ratio (Figure 4.5B). A high hepatic extraction by the non-cirrhotic livers of rosuvastatin was measured; 0.70 (IQR:0.69-0.83), which showed to be affected by cirrhosis (0.57 (IQR:0.42-0.67)). The hepatic extraction of digoxin, furosemide and metformin, which are low hepatic extraction ratio drugs, did not show to be affected by cirrhosis.

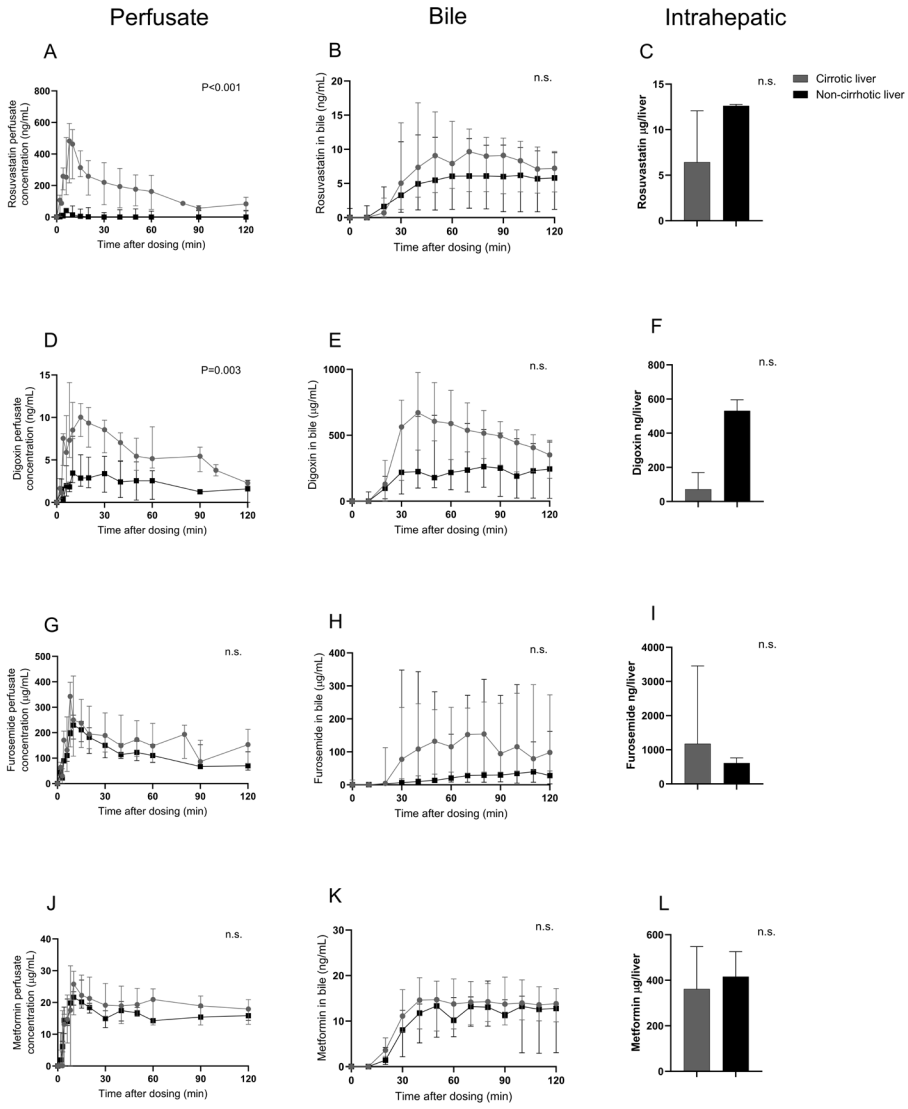

Figure 4.4 - Pharmacokinetic profiles of rosuvastatin, digoxin, metformin, and furosemide in cirrhotic and noncirrhotic perfused livers. Rosuvastatin (applied dose of 1.80 mg) (a) perfusate levels, (b) biliary excretion of rosuvastatin, and (c) intrahepatic rosuvastatin levels. Digoxin (applied dose of 0.11 mg) (d) perfusate levels, (e) biliary excretion of digoxin, and (f) intrahepatic digoxin levels. Furosemide (applied dose of 0.77 mg) (g) perfusate levels, (h) biliary excretion of furosemide, and (i) intrahepatic furosemide levels. Metformin (applied dose of 74.40 mg) (j) perfusate levels, (k) biliary metformin excretion, and (l) intrahepatic metformin levels. Data represent median and interquartile range in cirrhotic (n=7) and noncirrhotic livers (n=4) for perfusate and bile. There were five in the cirrhotic and three in noncirrhotic livers for intrahepatic data. Differences in AUC between groups were analyzed using the Mann–Whitney U test; P value is presented in the right corner of each graph. AUC, area under the concentration time curve; n.s., not significant.

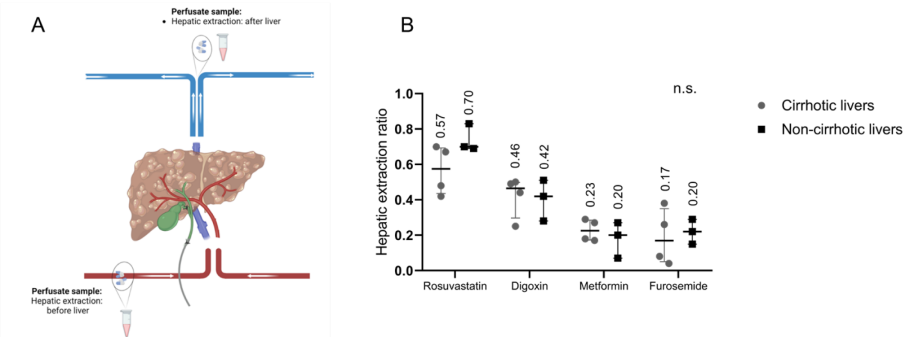

Figure 4.5 - Hepatic extraction of drug cocktail compounds. (a) Schematic representation of sample points before and after liver (b) hepatic extraction ratio of rosuvastatin, digoxin, metformin, and furosemide (*n*=3 noncirrhotic livers and *n*=4 cirrhotic livers). Differences between groups were analyzed using the Mann–Whitney *U* test; *P* value is presented in the right corner of each graph. n.s., not significant.

Increased risk of drug-drug interaction for rosuvastatin and digoxin

Figure 4.6 shows the results of the studies in which different drugs were used to inhibit the uptake and /or excretion of the drug cocktail from the previous section (Figure 6A). In both cirrhotic and non-cirrhotic livers, rosuvastatin and digoxin $AUC_{0\text{-}tau}$ and Cmax were increased upon co-administration of a perpetrator cocktail (Figure 4.6B,C). However, the drug-drug interaction, expressed as an increase in Cmax, and increase in AUCR (i.e. ratio AUC of victim drug with and without inhibitors over 120 min) was more profound but not significant in the non-cirrhotic livers than the cirrhotic livers. More specifically, the AUCR for rosuvastatin and digoxin was 5.6 (IQR: 3.1-13.3) and 8.1 (IQR: 4.6-20.5) respectively in non-cirrhotic livers compared to 1.4 (IQR: 0.9-1.9) and 2.2 (IQR: 1.3-3.5) respectively in cirrhotic livers. No increase in $AUC_{0\text{-}tau}$ and Cmax was observed for the low-hepatic extraction ratio drugs furosemide and metformin. The inhibition of biliary excretion (expressed in AUC ratio) of rosuvastatin and digoxin which are highly biliary excreted is shown in Figure 4.6D. The Pgp mediated biliary excretion of digoxin is shown to be inhibited as demonstrated by an AUCR ratio of 0.28 (IQR: 0.11-0.52) in cirrhotic livers and 0.66 (IQR: 0.12-1.14) in non-cirrhotic livers. Intrahepatic levels, demonstrated in Figure 4.6F, showed to be 6-fold increased in cirrhotic livers and 1.6-fold increased in non-cirrhotic livers upon co-administration of the inhibitors, which is in line with the inhibition of the biliary excretion.

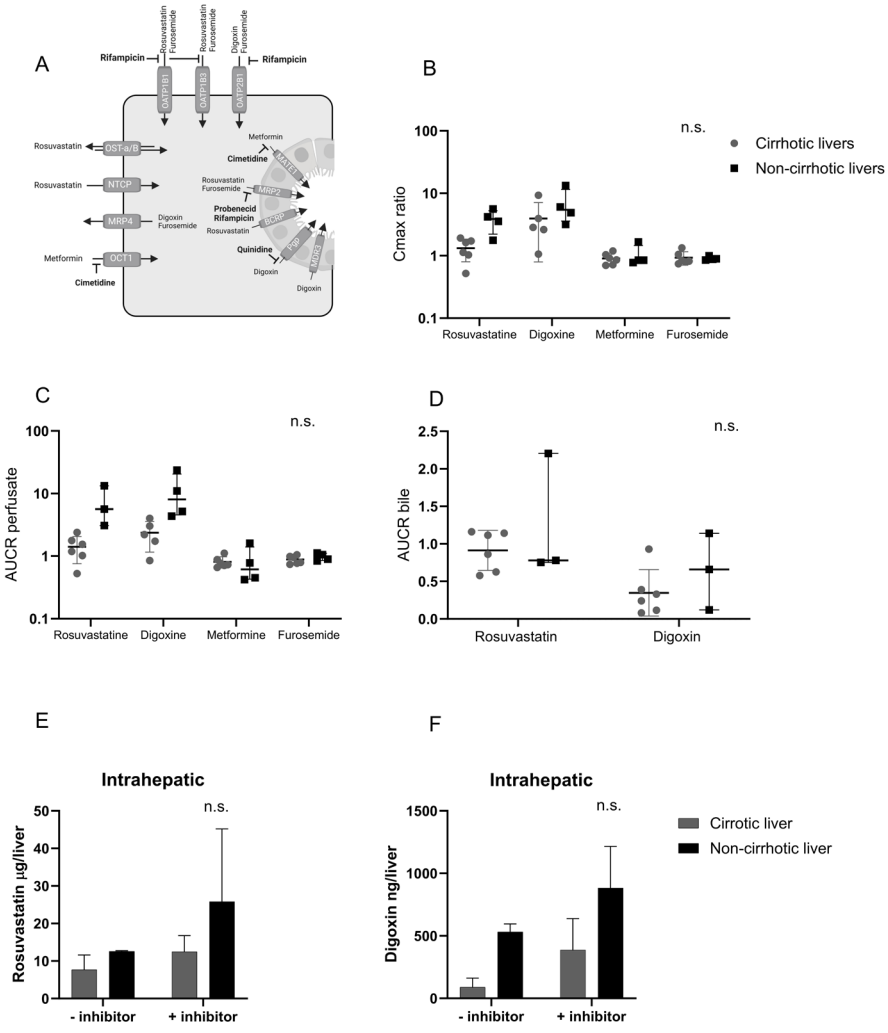

Figure 4.6 - Effect of drug inhibitor mix on hepatic clearance of rosuvastatin, digoxin, metformin, and furosemide. (a) Graphical representation of relevant hepatic drug transporters for the victim drugs (rosuvastatin, digoxin, metformin, and furosemide) and the applied perpetrators (quinidine, rifampicin, cimetidine, and probenecid). (b) Ratio of perfusate *C*max and (c) perfusate AUCR with and without applied perpetrator drugs for the cirrhotic and noncirrhotic livers. (d) Bile AUCR of digoxin and rosuvastatin with and without applied perpetrator drugs for the cirrhotic and non-cirrhotic livers. (e) Intrahepatic levels upon dosing inhibitor mix on rosuvastatin and (f) intrahepatic digoxin levels. Data represent median and interquartile range in cirrhotic (n=7) and noncirrhotic livers (n=4) for perfusate and bile, five in cirrhotic and three in noncirrhotic livers for intrahepatic data. Differences between groups were analyzed using the Mann–Whitney U test; P value is presented in the right corner of each graph. AUCR, area under the concentration time curve ratio; *C*max, maximum plasma concentration; n.s., not significant.

The BCRP mediated biliary excretion of rosuvastatin showed to be inhibited in the non-cirrhotic livers (0.78 (IQR:0.75-2.20)) while on average no inhibition of rosuvastatin in bile produced by cirrhotic livers was measured (0.98 (IQR:0.61-1.15)). Co-administration of the inhibitor mix showed to mildly increase the intrahepatic accumulation by 1.6-fold and 2-fold in cirrhotic and non-cirrhotic livers (Figure 4.6E). Metformin and furosemide showed to be minimally biliary excreted (range 1-3%), therefore no interaction in bile was presented here.

Discussion

Here we show for the first time the use of explanted human diseased livers as a model to assess hepatic extraction, biliary clearance and transporter function. We successfully perfused 7 cirrhotic livers and 4 non-cirrhotic livers for a period of 360 min, maintaining liver viability and functionality, as indicated by stable flow, bile production, proper histology pre- and post-perfusion, stable ALT values and stable gene expression throughout the perfusion.

The use of NMP has proven to be beneficial for organ transplantation[11,18] and NMP has become a widely accepted method to assess viability of the donor liver prior to transplantation[19,20]. Many criteria of hepatocellular and cholangiocellular function have been described (e.g. lactate clearance, perfusate ALT and biliary pH) to establish liver viability based on perfusion results and post-transplantation outcomes, demonstrating the robustness of the model in perfusion research[14-18]. The explanted cirrhotic livers perfused in this study met most of the criteria for hepatocellular function, except for lactate clearance and portal flow whereas other hemodynamic parameters did not show significant changes. As expected, portal flow was lower in cirrhotic livers compared to non-cirrhotic livers as a result of portal hypertension[21].

Unique advantages of the whole organ perfusion model is the dynamic environment; enabling to measure the hepatic extraction and the preservation of the biliary excretion route, thus allowing for the assessment of biliary excretion. The non-cirrhotic livers showed to rapidly take up rosuvastatin and digoxin from the perfusate with a hepatic extraction ratio of 0.70 and 0.42 respectively which are close to *in vivo* reported measures of 0.63 and 0.3 respectively[22,23]. In this study, hepatic extraction and clearance of rosuvastatin showed to be the most affected by cirrhosis as hepatic extraction decreased to

0.57 and a 190-fold AUC difference was observed. Rane et al.[24] reported that the clearance of hepatically cleared drugs with a high extraction ratio are related to blood flow and thus a major decrease in portal flow as in cirrhosis can dramatically affect the first passage across the liver[25,26]. However, changes in portal flow alone do not explain the 190-fold difference. Reduced uptake (C_{max}: 11.5-fold higher), as well as delayed elimination was observed. We hypothesize that decreased transporter abundance of OATP1B1/1B3 as reported in literature also contributed to the delayed elimination as we observed in the cirrhotic livers[27-29]. Hardly any studies are known regarding the effect of liver cirrhosis on for instance rosuvastatin pharmacokinetics. Only Simonson et al. 2003 reported the effect of advanced liver cirrhosis on rosuvastatin Cmax and AUC values for 2 patients[30]. This is substantiating the need for more knowledge regarding the role of cirrhosis in hepatic handling of drugs. *In vivo* studies demonstrated a high biliary excretion of rosuvastatin of approximately 76.8% as measured by fecal excretion[31]. The *ex vivo* non-cirrhotic livers showed a biliary excretion of 37% in 120 min, extrapolation of the data resulted in 77% total excretion of rosuvastatin which is in line with *in vivo* data. Interestingly, digoxin showed a relative high biliary clearance in cirrhotic (51%) and non-cirrhotic (17%) livers during 120 min of perfusion. *In vivo* studies have shown that digoxin is extensively renally eliminated (75%)[32]. However, multiple studies demonstrated that digoxin is highly involved in the enterohepatic circulation, thereby decreasing the *in vivo* fecal excretion of digoxin[33,34]. The two other compounds used in this study, furosemide and metformin, which are mainly renally cleared, showed a low hepatic extraction ratio and minor biliary excretion (≤3%) in both cirrhotic and non-cirrhotic which is in line with human *in vivo* data which showed that biliary eliminated was limited[35,36]. By showing the biliary excretion of two compounds which are mainly biliary excreted and two that are not/minorly excreted via the biliary route we demonstrated that the perfused liver retained its function while in the ex vivo environment. Interestingly, the percentage of biliary clearance was higher, for all compounds, in the cirrhotic perfused livers and lower intrahepatic levels of digoxin and rosuvastatin were measured. This might be due to an elevated bile flow which has been observed in patients cirrhosis and is confirmed in our model, resulting in a more efficiency biliary clearance[37]. Also, it has been reported for digoxin that Pgp levels are significantly elevated in cirrhosis which can contribute to a more efficient biliary clearance of digoxin[27].

The effect of drug-drug interactions in cirrhotic and non-cirrhotic livers was subsequently determined by using a cocktail of perpetrator drugs. The non-cirrhotic livers showed an increased AUCR for a drug-drug interaction with rosuvastatin (3.52) where values between 2.48–5.38 for rosuvastatin with rifampicin as inhibitor have been observed[38-40], showing good agreement with clinical data. Although it is observed that rifampicin can inhibit MRP2 and thereby limiting biliary excretion of rosuvastatin[41] we observed minimal inhibition at the biliary level. It is possible that the observed results are a consequence of inadequate portal dosing of rifampicin, as the perfusate concentration likely did not reach the desired levels. In our porcine perfusion we have measured C_{max} levels of 7.3 µM (n=10)[13], which is lower than 20 µM plasma levels in other clinical studies[38]. Digoxin, showed a high increase in AUCR upon dosing with inhibitors, which is potentially the result of inhibiting uptake via OATP (rifampicin as inhibitor) as described by Lau and co-authors[42]. A decrease in Pgp mediated biliary excretion was observed to an average inhibition of 0.64 in non-cirrhotic livers. This is the same inhibition we have observed in our porcine experiments. Since there is some variation between the human livers, we do recommend more replicates for future experiments. It remains difficult to compare to *in vivo* observations since a major part of the drug-drug interaction takes place at the intestinal level, when orally absorbed, thereby affecting the portal vein concentration. Still, the observations from this study showed that we could mimic a drug-drug interaction with digoxin in this perfusion model leading to an increased Cmax and AUCR.

Explanted livers obtained during orthotopic liver transplantation are currently only used for pathological assessment and subsequently discarded. While many preclinical and laboratory animal models try to mimic liver diseases as best as possible, many models fail due to a lack of translation to the human situation. This model can be widely applied in a variety of research settings, however implementation will only be feasible in a limited number of centers were liver transplantations are regularly performed. Considering the scarcity of explanted human livers for research purposes the utilization of porcine livers in early stages of drug development can prove to be a valuable approach as we have previously shown[13]. Although we have used a limited time-window perfusion, recent studies have shown the possibility to prolong organ perfusion duration even up to 7 days[19] which will broaden the applicability of liver perfusion.

Liver disease can affect the abundance of transporter proteins and/or metabolizing enzymes. In fact, multiple studies have analyzed liver biopsies from patients with liver disease showing alterations in expression of specific proteins relevant for pharmacokinetics[27-29,43]. For instance, Drozdzik et al., showed an increase in Pgp and multidrug resistance protein 4 (MRP4) and decreases in NTCP, OCT1 and OATP1B1 in patients with severe liver disease[27]. Although these studies already provided some hints towards altered pharmacokinetics and metabolism of drugs in patients with liver diseases, ex vivo perfusion of diseased livers offers a unique opportunity to directly study the effect of altered expression levels of transporter proteins and metabolizing enzymes. In this study we used known drug substrates for different important hepatic uptake and efflux transporters. Gaining insight into pharmacokinetic profiles of OATP1B1/1B3, Pgp, BCRP and OCT1 model compounds is a first step towards studying transporter functions in diseased liver. Additionally, for many drugs, dosing advice is currently incomplete for patients with cirrhosis because of lacking evidence or showing major interindividual differences. Studying drug pharmacokinetics using explanted human livers can serve as a basis to explore the differences in hepatic handling of drugs for patients with hepatic impairment even though to date it is yet too early to know what the exact place of this model is for clinical practice or drug development[44].

In conclusion, we demonstrated for the first time NMP of diseased human livers explanted during liver transplantation and discarded donor livers to study hepatic extraction, clearance, biliary excretion and drug-drug interactions. The ability to sample perfusate, bile and tissue during- and after dosing is a unique approach to gain insights into hepatobiliary processes, transporter function and transporter abundance.

Acknowledgements

We thank Elwin Verheij, René Braakman and Pieter Spigt for their help with the LCMS method development of the drug cocktail.

References

1. Franz CC, Egger S, Born C, Rätz Bravo AE, Krähenbühl S. Potential drug-drug interactions and adverse drug reactions in patients with liver cirrhosis. European journal of clinical pharmacology 2012;68:179-188.
2. Franz CC, Hildbrand C, Born C, Egger S, Rätz Bravo AE, Krähenbühl S. Dose adjustment in patients with liver cirrhosis: impact on adverse drug reactions and hospitalizations. European journal of clinical pharmacology 2013;69:1565-1573.
3. Rodighiero V. Effects of liver disease on pharmacokinetics. Clinical pharmacokinetics 1999;37:399-431.
4. Nevzorova YA, Boyer-Diaz Z, Cubero FJ, Gracia-Sancho J. Animal models for liver disease–A practical approach for translational research. Journal of hepatology 2020;73:423-440.
5. Guillouzo A. Liver cell models in in vitro toxicology. Environmental health perspectives 1998;106:511-532.
6. Du Y, Polacheck WJ, Wells RG: Bile Duct-on-a-Chip. In: Organ-on-a-Chip: Springer, 2022; 57-68.
7. Hassan S, Sebastian S, Maharjan S, Lesha A, Carpenter A-M, Liu X, Xie X, et al. Liver-on-a-chip models of fatty liver disease. Hepatology (Baltimore, Md.) 2020;71:733.
8. Melgert BN, Olinga P, Weert B, Slooff MJ, Meijer DK, Poelstra K, Groothuis GM. Cellular distribution and handling of liver-targeting preparations in human livers studied by a liver lobe perfusion. Drug metabolism and disposition 2001;29:361-367.
9. Schreiter T, Marquitan G, Darnell M, Sowa J-P, Bröcker-Preuss M, Andersson TB, Baba HA, et al. An ex vivo perfusion system emulating in vivo conditions in noncirrhotic and cirrhotic human liver. Journal of Pharmacology and Experimental Therapeutics 2012;342:730-741.
10. Villeneuve JP, Huet PM, Gariepy L, Fenyves D, Willems B, Cǒté J, Lapointe R, et al. Isolated perfused cirrhotic human liver obtained from liver transplant patients: a feasibility study. Hepatology 1990;12:257-263.
11. van Rijn R, Schurink IJ, de Vries Y, van den Berg AP, Cortes Cerisuelo M, Darwish Murad S, Erdmann JI, et al. Hypothermic machine perfusion in liver transplantation—a randomized trial. New England Journal of Medicine 2021;384:1391-1401.
12. Stopfer P, Giessmann T, Hohl K, Hutzel S, Schmidt S, Gansser D, Ishiguro N, et al. Optimization of a drug transporter probe cocktail: potential screening tool for transporter-mediated drug–drug interactions. British journal of clinical pharmacology 2018;84:1941-1949.
13. Stevens LJ, Zhu AZ, Chothe PP, Chowdhury SK, Donkers JM, Vaes WH, Knibbe CA, et al. Evaluation of normothermic machine perfusion of porcine livers as a novel preclinical model to predict biliary clearance and transporter-mediated drug-drug interactions using statins. Drug Metabolism and Disposition 2021;49:780-789.
14. de Vries Y, Matton AP, Nijsten MW, Werner MJ, van den Berg AP, de Boer MT, Buis CI, et al. Pretransplant sequential hypo-and normothermic machine perfusion of suboptimal livers donated after circulatory death using a hemoglobin-based oxygen carrier perfusion solution. American journal of transplantation 2019;19:1202-1211.
15. Brüggenwirth IM, van Leeuwen OB, Porte RJ, Martins PN. The emerging role of viability testing during liver machine perfusion. Liver Transplantation 2021.
16. Mergental H, Stephenson BT, Laing RW, Kirkham AJ, Neil DA, Wallace LL, Boteon YL, et al. Development of clinical criteria for functional assessment to predict primary nonfunction of high-risk livers using normothermic machine perfusion. Liver Transplantation 2018;24: 1453-1469.
17. van Leeuwen OB, de Vries Y, Fujiyoshi M, Nijsten MW, Ubbink R, Pelgrim GJ, Werner MJ, et al. Transplantation of high-risk donor livers after ex situ resuscitation and assessment using combined hypo-and normothermic machine perfusion: a prospective clinical trial. Annals of surgery 2019;270:906-914.
18. Boteon YL, Laing RW, Schlegel A, Wallace L, Smith A, Attard J, Bhogal RH, et al. Combined hypothermic and normothermic machine perfusion improves functional recovery of extended criteria donor livers. Liver transplantation 2018;24:1699-1715.

19. Eshmuminov D, Becker D, Bautista Borrego L, Hefti M, Schuler MJ, Hagedorn C, Muller X, et al. An integrated perfusion machine preserves injured human livers for 1 week. Nature biotechnology 2020;38:189-198.
20. Op den Dries S, Karimian N, Sutton M, Westerkamp A, Nijsten M, Gouw A, Wiersema-Buist J, et al. Ex vivo normothermic machine perfusion and viability testing of discarded human donor livers. American Journal of Transplantation 2013;13:1327-1335.
21. Bosch J, García-Pagán JC. Complications of cirrhosis. I. Portal hypertension. Journal of hepatology 2000;32:141-156.
22. Bergman E, Forsell P, Tevell A, Persson EM, Hedeland M, Bondesson U, Knutson L, et al. Biliary secretion of rosuvastatin and bile acids in humans during the absorption phase. European journal of pharmaceutical sciences 2006;29:205-214.
23. Hebert MF. Impact of pregnancy on maternal pharmacokinetics of medications. Clinical pharmacology during pregnancy 2013:17-39.
24. Rane A, Wilkinson G, Shand D. Prediction of hepatic extraction ratio from in vitro measurement of intrinsic clearance. Journal of Pharmacology and Experimental Therapeutics 1977;200: 420-424.
25. Delco F, Tchambaz L, Schlienger R, Drewe J, Krähenbühl S. Dose adjustment in patients with liver disease. Drug safety 2005;28:529-545.
26. Johnson TN, Boussery K, Rowland-Yeo K, Tucker GT, Rostami-Hodjegan A. A semi-mechanistic model to predict the effects of liver cirrhosis on drug clearance. Clinical pharmacokinetics 2010;49:189-206.
27. Drozdzik M, Szelag-Pieniek S, Post M, Zeair S, Wrzesinski M, Kurzawski M, Prieto J, et al. Protein abundance of hepatic drug transporters in patients with different forms of liver damage. Clinical Pharmacology & Therapeutics 2020;107:1138-1148.
28. Thakkar N, Slizgi JR, Brouwer KL. Effect of liver disease on hepatic transporter expression and function. Journal of pharmaceutical sciences 2017;106:2282-2294.
29. Wang L, Collins C, Kelly EJ, Chu X, Ray AS, Salphati L, Xiao G, et al. Transporter expression in liver tissue from subjects with alcoholic or hepatitis C cirrhosis quantified by targeted quantitative proteomics. Drug Metabolism and Disposition 2016;44:1752-1758.
30. Simonson S, Martin P, Mitchell P, Schneck D, Lasseter K, Warwick M. Pharmacokinetics and pharmacodynamics of rosuvastatin in subjects with hepatic impairment. European journal of clinical pharmacology 2003;58:669-675.
31. Martin PD, Warwick MJ, Dane AL, Hill SJ, Giles PB, Phillips PJ, Lenz E. Metabolism, excretion, and pharmacokinetics of rosuvastatin in healthy adult male volunteers. Clinical therapeutics 2003;25:2822-2835.
32. Iisalo E. Clinical pharmacokinetics of digoxin. Clinical pharmacokinetics 1977;2:1-16.
33. Doherty JE, Flanigan W, Murphy M, Bulloch R, Dalrymple G, Beard O, Perkins W, et al. Tritiated digoxin: XIV. Enterohepatic circulation, absorption, and excretion studies in human volunteers. Circulation 1970;42:867-873.
34. Ben-Itzhak J, Bassan HM, Shor R, Lanir A. Digoxin quinidine interaction: a pharmacokinetic study in the isolated perfused rat liver. Life sciences 1985;37:411-415.
35. Beermann B, Dalen E, Lindström B, Rosen A. On the fate of furosemide in man. European journal of clinical pharmacology 1975;9:57-61.
36. Graham GG, Punt J, Arora M, Day RO, Doogue MP, Duong J, Furlong TJ, et al. Clinical pharmacokinetics of metformin. Clinical pharmacokinetics 2011;50:81-98.
37. Erlinger S. Bile secretion. British medical bulletin 1992;48:860-876.
38. Mori D, Kashihara Y, Yoshikado T, Kimura M, Hirota T, Matsuki S, Maeda K, et al. Effect of OATP1B1 genotypes on plasma concentrations of endogenous OATP1B1 substrates and drugs, and their association in healthy volunteers. Drug metabolism and pharmacokinetics 2019;34:78-86.
39. Prueksaritanont T, Tatosian D, Chu X, Railkar R, Evers R, Chavez-Eng C, Lutz R, et al. Validation of a microdose probe drug cocktail for clinical drug interaction assessments for drug transporters and CYP3A. Clinical Pharmacology & Therapeutics 2017;101:519-530.

40. Takehara I, Yoshikado T, Ishigame K, Mori D, Furihata K-i, Watanabe N, Ando O, et al. Comparative study of the dose-dependence of OATP1B inhibition by rifampicin using probe drugs and endogenous substrates in healthy volunteers. Pharmaceutical research 2018;35: 1-13.
41. Kaneko K-i, Tanaka M, Ishii A, Katayama Y, Nakaoka T, Irie S, Kawahata H, et al. A clinical quantitative evaluation of hepatobiliary transport of [11C] dehydropravastatin in humans using positron emission tomography. Drug Metabolism and Disposition 2018;46:719-728.
42. Lau YY, Wu C-Y, Okochi H, Benet LZ. Ex situ inhibition of hepatic uptake and efflux significantly changes metabolism: hepatic enzyme-transporter interplay. Journal of Pharmacology and Experimental Therapeutics 2004;308:1040-1045.
43. Billington S, Ray AS, Salphati L, Xiao G, Chu X, Humphreys WG, Liao M, et al. Transporter expression in noncancerous and cancerous liver tissue from donors with hepatocellular carcinoma and chronic hepatitis C infection quantified by LC-MS/MS proteomics. Drug Metabolism and Disposition 2018;46:189-196.
44. Weersink RA, Bouma M, Burger DM, Drenth JP, Hunfeld NG, Kranenborg M, Monster-Simons MH, et al. Evaluating the safety and dosing of drugs in patients with liver cirrhosis by literature review and expert opinion. BMJ open 2016;6:e012991.

Supplementary materials

Table S4.1 - Composition of perfusate and continuous infusions.

Components	Quantity
Red blood cells (Sanquin)	4x 250 mL
Fresh Frozen plasma	4x 250 mL
Calcium gluconate (10%)	10 mL
Sodium bicarbonate 8.4% solution	To pH of 7.4
Heparin	1000 IU
Continuous infusion	
Fast-acting insulin	(10 U/mL; 1mL/h)
Taurocholate	(2% w/v; 10 mL/h)
Flolan	0.026mg/mL/h
Heparin	1041 U/h (1mL/h)
Aminoplasmal (B. Braun)	23 mL/h
Cernevit (Baxter)	22.5 mg/mL/h

Table S4.2 - General properties of drug cocktail (rosuvastatin, digoxin, metformin and furosemide) and drug cocktail inhibitor mix. Oral doses applied *in vivo* (mg), fraction absorbed and mg bolus applied to the portal vein of ex vivo perfused livers.

Substrate (victim drug)	Transporters involved	Metabolism	Fraction absorbed (%)	mg oral doses	mg bolus applied to *ex vivo* liver
Rosuvastatin	OATP1B1, OATP1B3, NTCP, MRP2, BCRP, OST-α/β	CYP2C9	50%	10 mg	1.80 mg
Digoxin	OATP2B1, Pgp MDR3	CYP3A4	81%	0.50 mg	0.11 mg
Metformin	OCT1, MATE1		53%	500 mg	74.20 mg
Furosemide	OATP2B1, OATP1B1, OATP1B3 MRP2		55%	5 mg	0.77 mg
Inhibitor mix					
Rifampicin	OATP1B1 OATP1B3 OATP2B1		95%	600 mg	67.7 mg
Quinidine	Pgp		80%	100 mg	22.4 mg
Cimetidine	OCT1 MATE1		72%	300 mg	59.89 mg
Probenecid	MRP2		50%	250 mg	25 mg

Table S4.3 - Details of the LC/MS conditions used for the analysis of digoxin, rosuvastatin, metformin and furosemide in perfusate and bile matrix.

Compound	Column	Mobile Phase A	Mobile Phase B	Time (min)	Mobile Phase B (%)		Flow (mL/min)
Perfusate and Tissue							
Digoxin	Waters	0.1%	0.1% Formic	0	100	0	0.6
Rosuvastatin	Acquity	Formic	Acid	0.50	100	0	
Metformin	UPLC BEH	Acid in	in	1.00	50	50	
Furosemide	C18; 2.1x50	MiliQ	Acetonitrile	1.50	5	95	
	mm, 1.7 µm;	water		2.20	5	95	
	art.nr			2.30	100	0	
	186002350			3.20	100	0	
Bile matrix							
Digoxin	Waters	0.1%	0.1% Formic	0	100	0	0.6
Rosuvastatin	Acquity	Formic	Acid	0.50	100	0	
Metformin	UPLC BEH	Acid in	in	6.50	40	60	
Furosemide	C18; 2.1x50	MiliQ	Acetonitrile	6.60	5	95	
	mm, 1.7 µm;	water		7.30	5	95	
	art.nr			7.40	100	0	
	186002350			8.30	100	0	

Table S4.4 - Details of the LC/MS conditions; Quantification of masses and retention times.

Compound	Rt (min) Perfusate/tissue	Rt (min) Bile	Exact mass	Polarity	Fragment	m/z
Metformin	0.27	0.28	129.1014	Pos	[M+H]+	130.1087
Metformin ISTD	0.27	0.27	135.1391	Pos	[M+H]+	136.1464
Digoxin	1.34	3.98	780.4296	Neg	[M+HCOOH-H]-	825.4284
Digoxin ISTD	1.34	3.97	783.4484	Neg	[M+HCOOH-H]-	828.4472
Furosemide	1.42	4.07	330.0077	Neg	[M-H]-	329.0004
Furosemide ISTD	1.42	4.04	335.0391	Neg	[M-H]-	344.0318
Rosuvastatin	1.48	4.83	481.1683	Neg	[M-H]-	480.1610
Rosuvastatin ISTD	1.57	5.41	468.1862	Neg	[M+HCOOH-H]-	513.1850

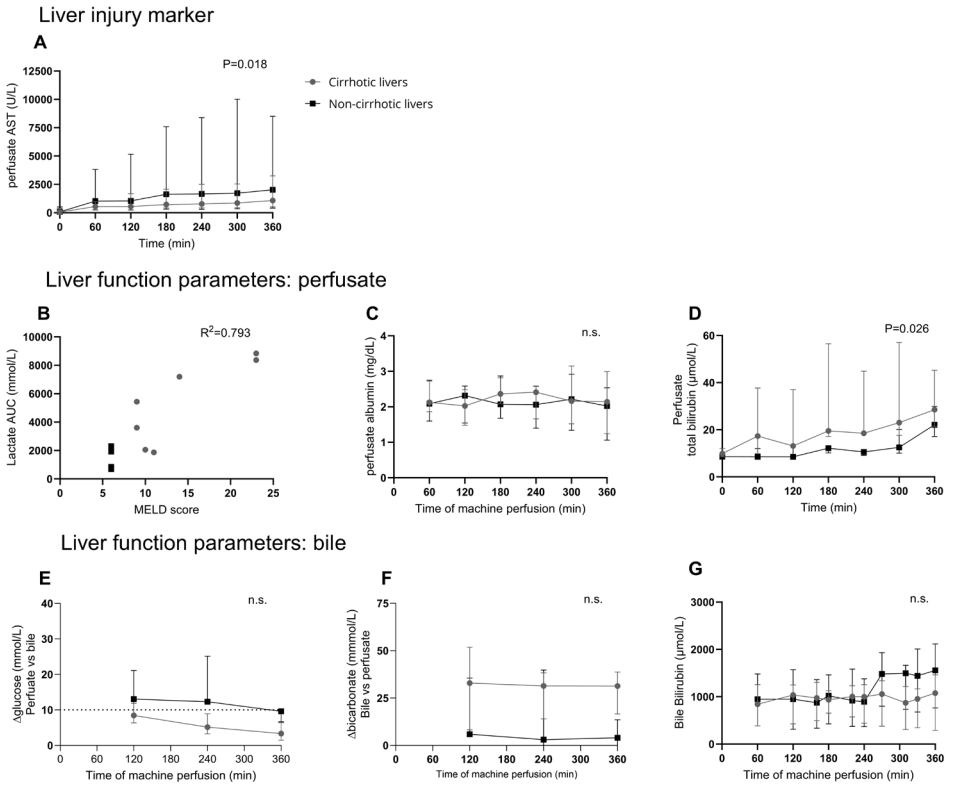

Figure S4.1 - Liver injury and liver function markers, measured in perfusate and bile during normothermic machine perfusion. Liver injury maker (A) Perfusate AST. Liver function parameters measured in perfusate, including; (B) relation of perfusate lactate AUC and MELD score, (C) albumin and (D) total bilirubin. Liver function parameters measured in bile; (E) Δglucose perfusate vs bile, (F) Δbicarbonate bile vs perfusate and (G) bile bilirubin levels during 360 min of perfusion. Data represents median and interquartile range in cirrhotic (n=7). and non-cirrhotic livers (n=4). Differences in AUC between groups were analyzed using the Mann-Whitney U test; p value is presented in right corner of each graph

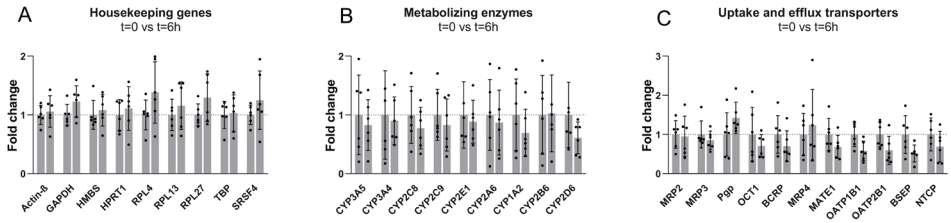

Figure S4.2 - mRNA expression of (A) housekeeping genes (B) CYP450 and (B) transporters during ex vivo normothermic perfusion. Tissue biopsies taken at t=0 hour were compared to t=6 hour. Data represents mean ±SD (n=6; cirrhotic/non-cirrhotic).

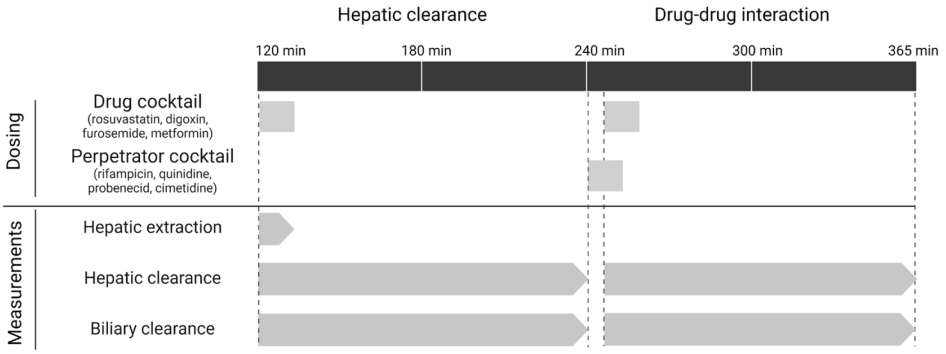

Figure S4.3 - Schematic representation of the experimental set-up for studying pharmacokinetics of a cocktail of drugs and the effects of drug-drug interactions. Stable liver perfusion was maintained in the first 120 min of perfusion. Between 120-130 min, the drug cocktail was infused into the portal vein (1mL/min), during this time the hepatic extraction of the drugs was measured. Hepatic clearance as well as biliary clearance was measured for 120 min (120 -240 min). Thereafter, at t=240 min, drug inhibitors were infused into the portal vein for 10 min (240–250). Between 245-255 the drug cocktail was infused into the portal vein to study drug-drug interactions. Perfusate and bile samples studying the extent of drug-drug interactions were taken between 245 and 365 min